Hemocytes/coelomocytes DNA content in five marine invertebrates: Cell cycles and genome sizes

Maja Fafanđel, Nevenka Bihari, Mirta Smodlaka, Sanda Ravlić

Center for Marine Research, Institut Ruđer Bošković
HR – 52 210 Rovinj, Croatia

Correspondence:
M. Fafanđel
«Ruđer Bošković» Institute
Center for Marine Research,
G. Paliaga 5, HR – 52 210 Rovinj, Croatia
Tel.: + 385 52 804 718
Fax.: + 385 52 813 496
E – mail: maja@cim.irb.hr

Running title: DNA content in marine invertebrates

Abstract The hemocytes/coelomocytes DNA content in five selected marine invertebrates (sea mouse *Aphrodita aculeata*, spiny crab *Maja crispata*, sea star *Echinaster sepositus*, sea urchin *Paracentrotus lividus*, tunicate *Phallusia mammillata*) was investigated by flow cytometry. The cell cycle analyses identified sea mouse coelomocytes as proliferating cells and revealed that spiny crab hemocytes and sea urchin coelomocytes complete their division in the hemolymph and coelom respectively. The genome sizes of sea mouse and spiny crab are reported for the first time. The diploid DNA content (2C) in sea mouse *A. aculeata* is 1.24 pg, of spiny crab *M. crispata* 7.76 pg, red starfish *E. sepositus* 1.52 pg and of sea urchin *P. lividus* 1.08 pg. The mean diploid DNA content in tunicate *P. mammillata* was 0.11 pg with a high interindividual variability (45 %). The presented results provide a useful database for future studies in the field of invertebrate physiology, ecotoxicology, biodiversity, species conservation and phylogeny.

Keywords: Cell cycle; coelomocytes; DNA content; genome size; hemocytes; marine invertebrates

Abbreviations: DAPI – 4',6 - diamidino-2-phenylindole; FSC – forward scatter fluorescence; FL6 – DAPI fluorescence; GS – genome size

Introduction

Invertebrates play a very important role in the maintenance of the health of marine ecosytems: filter feeders help maintain water quality, scavengers remove dead animals, and infaunal marine invertebrates improve sediment quality. Accordingly, benthic filter/sediment feeders are susceptible to environmental contamination and have become of interest as bioindicators. When exposed to environmental challenges, invertebrates modify the metabolic activity of different organs depending on involvement of these organs in the corresponding physiological processes. As primary immune effectors that respond to stress conditions, injuries, host invasion and cytotoxic/genotoxic agents, hemocyte/coelomocytes of benthic invertebrates have been used for the monitoring of environmental conditions (Matranga et al. 2000, Radford et al. 2000, Coteur et al. 2002, Bihari & Fafanđel 2004). They are free circulating cells that are easily collected and analysed by flow cytometry.

Flow cytometry has been used as a tool to investigate the cellular machinery in blood cells of invertebrates for the last 15 years. Analyses have focused on functions linked to innate immunity and on the sensitivity of cells to a particular stress or toxic agents. In addition, analyses provide information about the phenotype of a given invertebrate cell, the capacity to perform a given function or the response to a given stress (reviewed by Cossarizza et al. 2005). Namely, flow cytometric analyses have enabled the determination of phagocytic activity in starfish amoebocytes challenged by bacteria (Coteur et al. 2002), determination of the DNA content in mussel hemocytes (Rodriguez-Juiz et al. 1996) as well as alterations in the cell cycle as a result of either acute or cumulative genotoxic effects of the surrounding environment (Bihari et al. 2003). The DNA content is a marker of cellular maturity in the cell cycle since the frequency of cells in G0, S and G2 phases could determine the proliferative status of the investigated cells. When measurement is performed with an internal standard of known DNA content, flow cytometry provides information about genome size. Genome size is an important feature that defines the genetic characteristic of a species by determining its capacity to undergo evolutionary changes (Cavalier-Smith 1985). It is also an ecological parameter relevant for the determination of the development rate in poikilothermal animals and for species participation in niche-partitioning (Sessions & Larson 1987, Bennett 1987).

In this study blood cells of five benthic invertebrate species belonging to four different phyla (Annelida - sea mouse *Aphrodita aculeata*, Arthropoda - spiny crab *Maja crispata*, Echinodermata - sea star *Echinaster sepositus*, sea urchin *Paracentrotus lividus*, and Tunicata - *Phallusia mammillata*), that are all common in the Northern Adriatic, were investigated. In

many invertebrates, the hematopoietic/cytopoietic organs as well as the blood cells proliferation and maturation dynamics is unknown. Analyses of the DNA content and cell cycle of various tissues could be helpful in resolving this problem. Therefore the DNA content of hemocytes/coelomocytes for the five invertebrate species was analysed by flow cytometry. The cell cycles and the genome sizes were calculated and discussed. The presented results provide a useful database for future studies in the field of invertebrate physiology, ecotoxicology, biodiversity, species conservation and phylogeny.

Materials and methods

Experimental organisms

Specimens of marine invertebrates were collected in the vicinity of Rovinj, Northern Adriatic, Croatia at the depth of 2 – 20 m by (i) fish – trap: spiny crab *Maja crispata*, Risso (Arthropoda (class Crustacea): Decapoda: Majidae); (ii) diving: sea urchin *Paracentrotus lividus*, Lamarck (Echinodermata: Echinoidea: Echinidae) and (iii) dredging: sea mouse *Aphrodita aculeata*, Linneaus (Annelida: Polychaeta: Aphroditidae), red starfish *Echinaster sepositus*, Gray (Echinodermata: Stelleroidea: Asteriidae) and tunicate *Phallusia mammillata*, Cuvier (Tunicata: Ascidiacea: Ascidiidae). Collected specimens were immediately brought to the laboratory in aerated sea water and acclimated in aquaria with running sea water at the field temperature at least 24 h before analyses took place.

Sample preparation and nucleus staining

The crab hemolymph was sampled from the basal region of the large leg. The sea urchins were bled through a cut in a peristomal membrane. The sea mouse coelomic fluid was collected between muscles of the body wall and gut. The sea star coelomocytes were collected by cutting the tip of one arm and draining the coelomic fluid. The tunicate coelomic fluid was collected from the pericardium. To prevent clotting as a quick response to non-self materials hemolymph and coelomic fluid were immediately placed in Vacuettes® containing sodium citrate (Greiner bio-one GmbH, Germany). For flow cytometry analysis 100 µl of each sample were mixed with 2 ml of commercial 4',6 – diamidino-2-phenylindole (DAPI) solution (Cystain DNA 1 step, Partec, Germany) and the nuclei were stained for 10 min. at room temperature. Mussels (*Mytilus galloprovincialis*) sperm was prepared according to Elston et al. (1990) and used as an internal size standard of known DNA content for genome size estimation.

Flow cytometry

DAPI (Partec, Germany) – stained nuclei were analysed using a PAS III flow cytometer (Partec) at a flow rate 200 – 400 cells/sec with a 100 W mercury lamp under standard conditions (Partec) for detection of DAPI signals (FL6). As an instrument calibration standard, trout erythrocytes were used. For cell cycle measurement 20 000 nuclei of 10 specimens for each species were analysed. During the analysis of each species, the photomultiplier voltage was adjusted to maintain the histogram 2C peak at a constant fluorescence value. The results were displayed as histograms of the number of nuclei in each of the 264 channels (linear amplified fluorescence) where channel number was proportional to fluorescence intensity. For genome size analysis, measurements were rerun after adding 10 µl of mussel sperm as an internal reference standard. During the analysis of each species, the photomultiplier voltage was adjusted to maintain the histogram 1C peak of internal standard at a constant fluorescence value. Channel number data of 2C nuclei for each species and of the internal standard were used to compute genome size. The genome size (GS) was calculated from fluorescence intensity (FL6 arbitrary units) as $GS = FL6_{sample} / FL6_{mussel\ sperm}$ x 1.92 pg where 1.92 corresponds to the haploid genome size of mussel *Mytilus galloprovincialis* sperm (Rodríguez-Juíz et al. 1996). Acquisition, control and cell cycle analysis of the samples were carried out with a software system FloMax (Quantum Analysis GmbH, Germany).

Microscopic analysis

DAPI (Partec)-stained nuclei prepared for flow cytometry analyses were also used for microscopic analyses. Additionaly, red starfish coelomocytes (2 ml) were stained with a 100 µl 1 µg / ml DAPI (Sigma, D-9542) solution. Samples were observed at 1000x under UV light on a NIKON Microphot – FXA/SA epifluorescence microscope (100 W operating with mercury lamp and the following filter set: EX 330-380 excitation filter, DM dichroic mirror, BA 420 barrier filter).

Results and Discussion

Cell cycle

The fluorescence histogram of DAPI stained nuclei of sea mouse *Aphrodita aculeata* coelomocytes is presented in Fig. 1A. Four populations of nuclei are represented in histogram: population at 30.17 (peak 1), at 41.26 (peak 2), at 59.92 (peak 3) and at 78.13

(peak 4) channel numbers means. Ratios between the means of peak 3 and 1 (1.99) as well as between peak 4 and 2 (1.89) are indicative for two cell cycles of two nuclear populations with different DNA content. Thus, peak 1 represents G0/G1 cell cycle stage of one nuclear type with corresponding G2/M stage in peak 3. Similarly, peak 2 represents G0/G1 cell cycle stage of other nuclear type with corresponding G2/M stage in peak 4. The presence of two nuclear types was confirmed with microscopic analysis of DAPI stained nuclei (Fig. 1B). High relative proportion of nuclei in peak 2 (47 – 88 %) indicates them as a population of the sea mouse coelomocytes nuclei in G0/G1 phase. Nuclear population in peak 1 could originate from sea mouse tissue rather than coelomocytes or they could be cells of some other species. Variations in the DNA content of different tissues have been reported by Tiersch & Wachtel (1993). Collection of coelomocytes with syringe could cause contamination with other tissues such as skin or muscle. When blood cells and other tissues from the same animal were mixed, the sample displayed fluorescence distributions with pronounced shoulders or in some cases separate peaks. It is also possible that among sea mouse circulating coelomocytes two different cellular types with different DNA content are present. In moth *Manduca sexta* plasmatocytes were found to have higher ploidy levels than granular cells (Nardi et al. 2003). Although the S phase and cell cycle could not be determined due to the overlapping of two nuclear populations, presence of G2/M phase (peak 4) indicated that sea mouse coelomocytes divided or completed division in the coelom. High percentage (20 %) of proliferating cells in S, G2 and M phases of the cell cycle were quite common in Annelids (Homa et al. 2008) suggesting that sea mouse coelomocytes proliferate in the coelom.

Figure 2A shows the distribution of DAPI stained nuclei of spiny crab *Maja crispata* hemocytes. A single peak corresponding to nuclei in G0 phase was representative for 9 of 10 investigated specimens. Such profile is indicative for non dividing cell populations of hemocytes during blood circulation. In decapods the hemocytes differentiate in the hematopoietic organ from where they are released into circulation as mature hemocytes. Nuclear distribution in the different phases of the cell cycle was observed for one specimen. 2D forward scatter/DAPI plot (FSC/FL6) clearly shows presence of nuclei in G0/G1, S and G2/M phase (Fig. 2B). This suggests that spiny crab hemocytes either divided or completed division in the hemolymph. In both cases the need for extra hemocytes in the hemolymph was indicative. Karyokinesis was confirmed with microscopic analysis of DAPI-stained nuclei (Fig. 2C). The increase in the abundance of circulating hemocytes (granulocytes) capable of division just after molting and their subsequent movement into the epithelium of the exoskeleton in decapoda, lobster *Homarus americanus* was described (Factor 1995).

The result of the flow cytometry analyses of red starfish *Echinaster sepositus* coelomocytes DAPI-stained nuclei is presented in Fig. 3A. The distribution of the nuclei displayed two distinguishable peaks. The absence of peaks representing dividing nuclei in S and G2/M phases was in accordance with the previously published reports that no mitotic division of coelomocytes has ever been observed (Chia & Xing 1996) and that all coelomocytes in starfish originate from the coelomic epithelium (Bossche & Jangoux 1976). The ratio between DNA content in peak 2 and peak 1 (5) was indicative for the presence of an additional nuclear type from some unknown source. The presence of two nuclear types was confirmed by microscopic analysis of DAPI-stained nuclei (Fig. 3B). Since some coelomocyte types (phagocytes) are very efficient in recognising foreign particles (bacteria, cell debris, foreign cells…) (Smith 1981) unknown nuclei might represent engulfed particles in the red starfish phagocytes. When challenged by bacteria, starfish (*Asterias rubens*) amoebocytes were engaged in phagocytosis in a large proportion (70 %) (Coteur et al. 2002). When starfish *E. sepositus* cells were stained with DAPI, foreign nuclei (FN) were found inside the coelomocytes (Fig. 3C) confirming the presence of a phagocytic activity even in the unchallenged starfish. This finding was not surprising since phagocytosis is an important feature of the immune response of all multicellular invertebrates representing the first line of internal defence (Greenberg 1989).

The fluorescence histogram of DAPI-stained nuclei of sea urchin *Paracentrotus lividus* coelomocytes is presented in Fig. 4A. The distribution of the nuclei is represented by two peaks: a prominent one (2C) and a weak one (4C) with double the DNA content of the prominent peak. No important nuclear fraction between 2C and 4C peaks, which could have been assigned to nuclei in the S phase of proliferation, was detected. Since doublets were excluded during flow cytometric analysis 4C nuclei might be considered as nuclei in G2/M phase. Sea urchins coelomocytes do not divide but derive from progenitor cells at multiple sites (the visceral peritoneum, peritome peritoneum, hydrocoel peritoneum, Polian vesicle, haemal strands and dermal connective tissue) (Holland et al. 1965). The detected absence of proliferating nuclei in S phase and presence of 2.09 ± 0.35 % (10) 4C nuclei in coelomic fluid suggests that the coelomocyte's division, that started elsewhere, is completed in the coelom. Microscopic analysis of DAPI-stained nuclei (Fig. 4B) confirmed karyokinesis in the coelom.

The fluorescence histogram of tunicate *Phallusia mammillata* DAPI-stained coelomocytes nuclei is presented in Fig. 5A, while microscopic analysis of DAPI-stained nuclei is presented in Fig. 5B. The distribution of the nuclei displayed only one peak at the detection limit and the cell cycle of tunicate coelomocytes was not detected.

DNA content

There are two approaches for the determination of 2C DNA content for a given organism: analysis of the DNA extracted from a large number of cells and the measurement of individual nuclei. The measurement of individual nuclei can be easily performed by flow cytometry. Since flow cytometry measures the relative DNA content, the genome size of an unknown sample can be determined only after comparison with nuclei from a reference sample, of which the genome size is known. The relative fluorescence histograms of five invertebrate species, analyzed together with mussel *Mytilus galloprovincialis* sperm as an internal reference standard, are presented in Fig. 6. Since the sea urchin florescence signals overlap with the mussel sperm signal, mussel sperm could not be used for the calculation of sea urchin DNA content and mussel hemocytes were used instead. The DNA content of the diploid nuclei of *M. galloprovincialis* has been previously determined as 3.84 pg on the basis of comparison with *Capsicum annuum* (Rodriguez-Juiz 1996).

The mean DNA content and the statistical description of the distribution of DNA content for analysed individuals within each species are presented in Table 1. The variations between individuals within each of the populations (sea mouse, spiny crab, red starfish and sea urchin) were below 5 %. This is similar to the range already reported for cyprinid fish and bivalves (Gold & Price 1987, Rodriguez-Juiz 1996). Observed intraspecific variations in nuclear DNA content could be linked to chromosomal polymorphism reorganization, genome reordination and varying levels of constitutive heterochromatin (Gold & Price 1987). The diploid DNA content (2C) of sea mouse *A. aculeata* was 1.24 pg. This is the first record of the genome size of any species belonging to the family Aphroditidae. According to detailed references in Animal Genome Size Database (http://www.genomesize.com), there is a great heterogeneity in genome size (0.11 - 7.2 pg) among the species of the order Phyllodocida. The genome size of sea mouse is more similar to the species in the families Silidae and Hesonidae (< 1.0 pg per haploid) than to Glyceridae or Nephtidae, where for some species haploid genome size is 7.2 pg (Conner et al. 1972, Gambi et al. 1997). The diploid DNA content (2C) of spiny crab *M. crispata* was 7.76 pg. This is in the range of the genome size of spider crabs *Libinia spp* (haploid: 2.21 – 4.55 pg) belonging to the same Majidae family (Bachmann & Rheinsmith 1973, Rheinsmith et al. 1974, Vaughn 1975). The diploid DNA content (2C) of starfish *E. sepositus* is 1.52 pg, a figure represented in the range belonging to the familiy Asteriidae (haploid: 0.58 – 0.7 pg) (Hinegardner 1974). The diploid DNA content (2C) of sea urchin *P. lividus* is 1.08 pg. The difference from the previously reported haploid genome size of the same species (0.9 pg) (White 1961) could be attributed to different methodological

approaches. The mean diploid DNA content (2C) of tunicate *P. mammillata* is 0.11 pg. The high interindividual variability in the DNA content of tunicate (45 %) could arise from the small genome size that results in a low fluorescent signal (at the limit of the instrument detection) obtained after DAPI-staining. For more accurate determination of such small DNA genome sizes as those found among tunicates (Jeffery 2002), more sensitive staining methods are recommended.

Conclusions

1. Flow cytometry analyses of DAPI-stained nuclei identified the sea mouse *A. aculeata* coelomocytes as proliferating cells.
2. Fluorescence microscopy of DAPI-stained cells identified the presence of phagocytic activity in unchallenged red starfish *E. sepositus*.
3. Evidence of karyokinesis of both spiny crab hemocytes and sea urchin coelomocytes reveals that their division is completed in the hemolymph and coelom respectively.
4. The diploid DNA content (2C) in sea mouse *A. aculeata,* spiny crab *M. crispata,* red starfish *E. sepositus,* and sea urchin *P. lividus* is 1.24, 7.76, 1.52 and 1.08 pg respectively.
5. DNA content of the sea mouse *A. aculeata* and spiny crab *M. crispata* are the first records of their genome sizes. Furthermore, the DNA content of the sea mouse *A. aculeata* is the first genome size record among the species in the Aphroditidae family.

Acknowledgement

The Croatian Ministry of Science, Education and Sport funded this investigation (Project 098-2705-2725).

References

Bachmann K. & Rheinsmith E.L. 1973. Nuclear DNA amounts in Pacific Crustacea. Chromosoma **43:** 225-236.

Bennett M.D. 1987. Variation in genomic form in plants and its ecological implications. New Phytol. **106:** 177-200.

Bihari N., Mičić M., Batel R. & Zahn R.K. 2003. Flow cytometric detection of DNA cell cycle alterations of hemocyte of mussels (*Mytilus galloprovincialis*) off the Adriatic coast, Croatia. Aquat. Toxicol. **64:** 121-129.

Bihari N. & Fafanđel M. 2004. Interspecies differences in DNA single strand breaks caused by benzo(a)pyrene and marine environment. Mutat. Res. **552:** 209-217.

Bossche J.P. & Jangoux M. 1976. Epithelial origin of starfish coelomocytes. Nature **261:** 227-228.

Cavalier-Smith T. 1985. The evolution of genome size. John Wiley and Sons, New York

Chia F-S. & Xing J. 1996. Echinoderm coelomocytes. Zool. Stud. **35:** 231-254.

Conner W.G., Hinegardner R. & Bachamann K. 1972. Nuclear DNA amounts in polychaete annelides. Experientia **28:** 1502-1504.

Cossarizza A., Pinti M., Troiano L. & Cooper E.L. 2005. Flow cytometry as a tool for analysing invertebrate cells. Invertebr. Surv. J. **2:** 32-40.

Coteur G., DeBecker G., Warnau M., Jangoux M. & Dubois P. 2002. Differentiation of immune cells challenged by bacteria in the common Europian starfish, *Asterias rubens* (Echinodermata). Eur. J. Cell Biol. **81:** 413-418.

Elston R.A., Drum A.S. & Allen S.K. Jr 1990. Progressive development of circulating polyploid cells in Mytilus with haemic neoplasia. Dis. Aquat. Org. **8:** 51-59.

Factor J.R. (ed.) 1995. Biology of the lobster *Homarus americanus*, Academic Press, San Diego.

Gambi M.C., Ramella L., Sella G., Protto P. & Aldieri E. 1997. Variation in genome size of benthic polychaetes: Systematic and ecological relationships. J. Mar. Biol. Ass. UK **77:** 1045-1057.

Gold J.R. & Price H.J. 1987. Genome size variation in North American minnows (Cyprinidae) I. Distribution of the variation in five species. Heredity Lond. **54:** 197-305.

Greenberg S.S. 1989. Immunity and survival. Human Sciences Press, New York pp. 19-34.

Hinegardner R.1974. Cellular DNA content of the Echinodermata. Comp. Biochem. Physiol. **49B:** 219-226.

Holland N.D., Phillips J.H. & Giese AC 1965. An autographic investigation of coelomocyte production in the purple sea urchin (*Strongylocentrotus purpuratus*). Biol. Bull. **128:** 259-270.

Homa J., Bzowska M., Klimek M. & Plytycz B. 2008. Flow cytometric quantification of proliferating coelomocytes non-invasively retrieved from earthworm *Dendrobaena veneta*. Develop. Comp. Immunol. **32:** 9-14.

Jeffery W.R. 2002. Ascidian gene-expression profiles. Gen. Biol. **3,10:** 1030.1-1030.4.

Matranga V., Toia G., Bonaventura R. & Müller W.E.G. 2000. Cellular and biochemical responses to environmental and experimentally induced stress in sea urchin coelomocytes. Cell Stress Shaper. 5: 113-120.

Nardi, J. B., Pilas, B., Ujhelyi, E., Garsha, K. & Kanost, M. R. 2003. Hematopoietic organs of *Manduca sexta* and hemocyte lineages. Dev. Genes. Evol. **213**: 477-491.

Radford J.L., Hutchinson A.E., Burandt M. & Raftos D.A. 2000. Effects of metal – based environmental pollutants on tunicate hemocytes. J. Invertebr. Pathol. **76:** 242-248.

Rheinsmith E.L., Hinegardner R. & Bachmann K. 1974. Nuclear DNA amounts in Crustacea. Comp. Biochem. Physiol. **48B:** 343-348.

Rodríguez-Juíz, A.M., Torrado M. & Méndez J. 1996. Genome-size variation in bivalve molluscs determined by flow cytometry. Mar. Biol. **126:** 489-497.

Schreiber A., Stürenberg F. & Storch V. 1994. DNA content in blood cells of *Halicryptus spinulosus,* a species of the phylum Priapulida. Naturwissenschaften **80:** 455-456.

Sessions S.K. & Larson A. 1987. Developmental correlates of genome size in plethodontid salamanders and their implications for genome size. Evolution **41:** 1239-1251.

Smith V.J. 1981. The echinoderms. In: Invertebrate blood cells. Eds. Ratcliffe N.A., Rowley A.F., Academic Pres, London, pp. 513-562.

Tiersch T.R. & Wachtel S.S. 1993. Sources of error in screening by flow cytometry for the effects of environmental mutagens. Environ. Toxicol. Chem. **12:** 37-42.

Vaughn J.C. 1975. DNA reassociation kinetics and chromosome structure in the crabs *Cancer borealis* and *Libinia emarginata*. Chromosoma **50:** 243-257.

White M.J.D. 1961. The Chromosomes, John Wyley and Sons, New York.

Table and figure legends

Table 1. Descriptive statistics of genome size variation within 5 species of marine invertebrates calculated from distribution of DNA values of 10 specimens.

Fig. 1. Sea mouse *Aphrodita aculeata* coelomocytes. A) DAPI-fluorescence (FL6) distribution defining 4 nuclear populations. B) Photomicrograph of DAPI-stained nuclei. Bar: 10 µm. Numerous bacteria are visible.

Fig. 2. Spiny crab *Maja crispata* hemocytes. A) DAPI-fluorescence distribution defining 1 nuclear population (9 of 10 specimens). B) cell cycle detected by bivariate histogram of DAPI-fluorescence (FL6) versus fluorescence side scatter (FSC) in 1 of 10 specimens. C) Photomicrograph of DAPI-stained nuclei. Bar: 10 µm.

Fig. 3. Red starfish *Echinaster sepositus* coelomocytes. A) DAPI-fluorescence (FL6) distribution defining 2 nuclear populations. B) Photomicrograph of two types of DAPI-stained nuclei. Bar: 10 µm. C) Photomicrograph of DAPI-stained coelomocytes. DNA-containing fluorescent particles (FN) are visible beside nucleus (N). Bar: 10 µm.

Fig. 4. Sea urchin *Paracenthrotus lividus* coelomocytes. A) DAPI-fluorescence (FL6) distribution defining 2 nuclear populations. B) Photomicrograph of DAPI-stained nuclei during karyokinesis. Bar: 10 µm.

Fig. 5. Tunicate *Phallusia mammillata* coelomocytes. A) DAPI-fluorescence (FL6) distribution defining 1 nuclear population. B) Photomicrograph of DAPI-stained nuclei. Bar: 10 µm.

Fig. 6. Flow cytometric fluorescence – distribution defining nuclear populations of five invertebrate species. In each analysis reference mussel nuclei (MS – mussel sperm or MH – mussel hemocytes) was included.

1

2

Species	DNA content (2C) / pg	Range	CV
Aphrodita aculeata	1.24 ± 0.06	1.15 – 1.30	4.8
Maja crispata	7.76 ± 0.10	7.63 – 7.91	1.3
Echinaster sepositus	1.52 ± 0.03	1.46 – 1.54	2.0
Paracenthrotus lividus	1.08 ± 0.02	1.05 – 1.12	4.6
Phallusia mammillata	0.11 ± 0.05	0.07 – 0.14	45

3

4

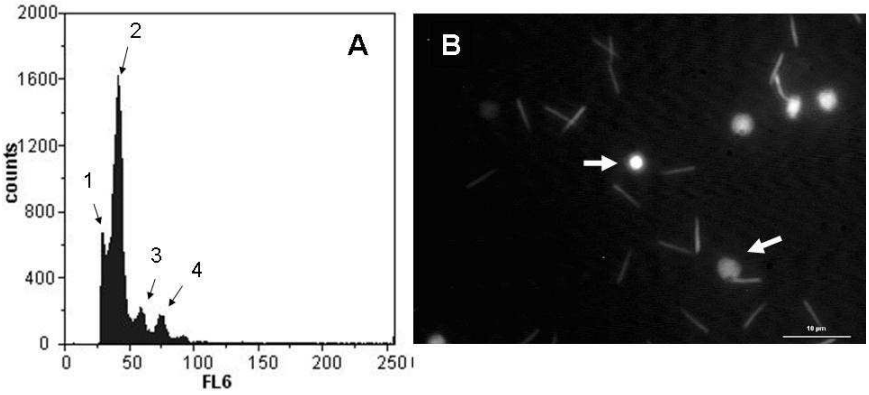

Figure 1.

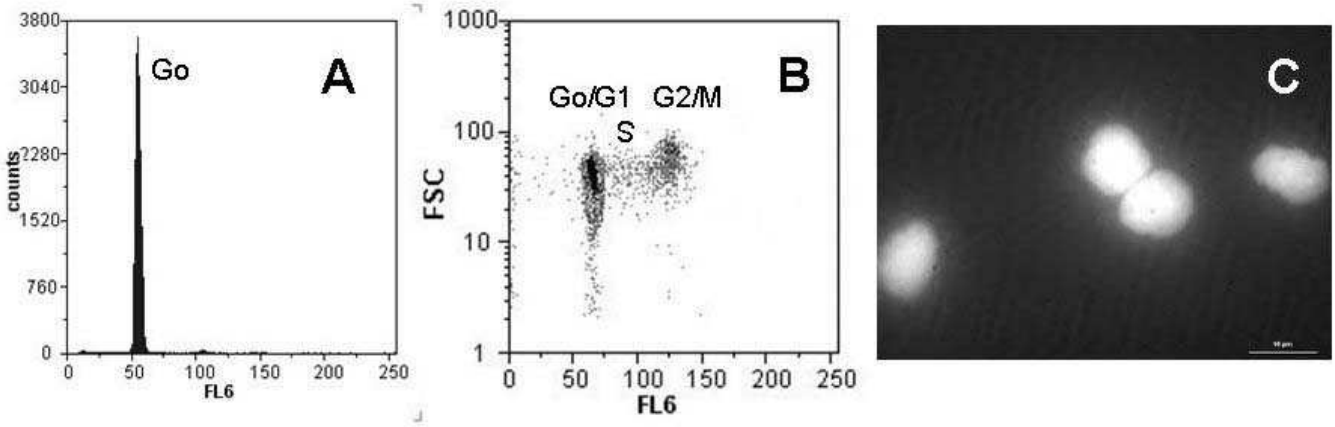

Figure 2.

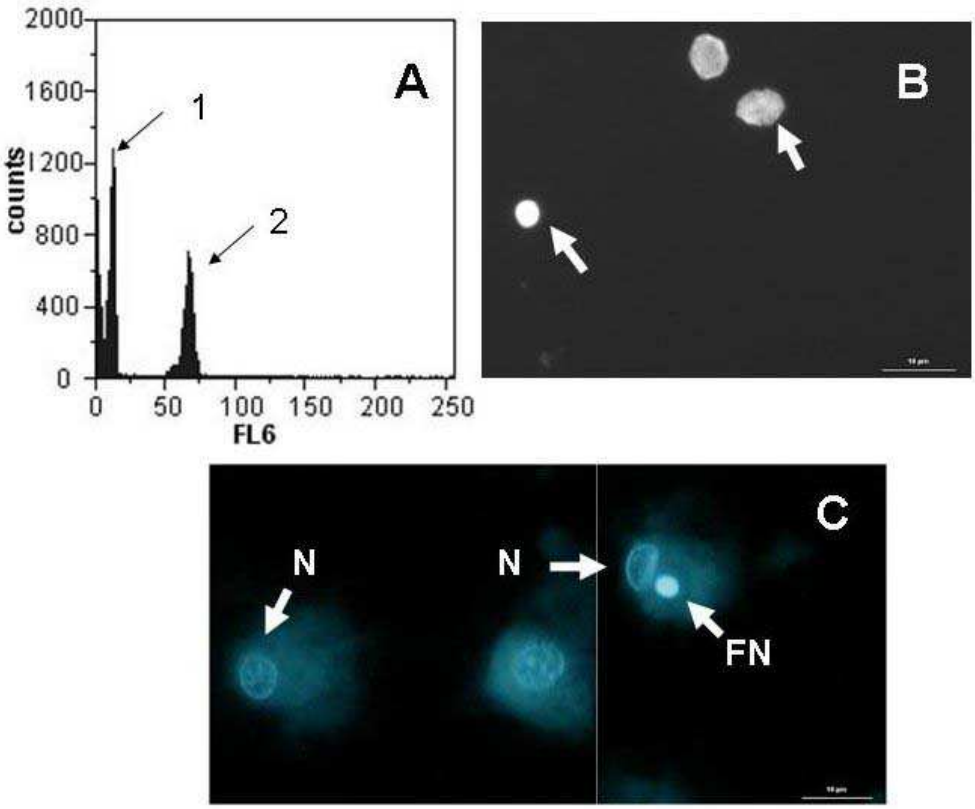
A
B
C
1
2
counts
FL6
2000
1600
1200
800
400
0
0
50
100
150
200
250
N
N
FN

Figure 3.

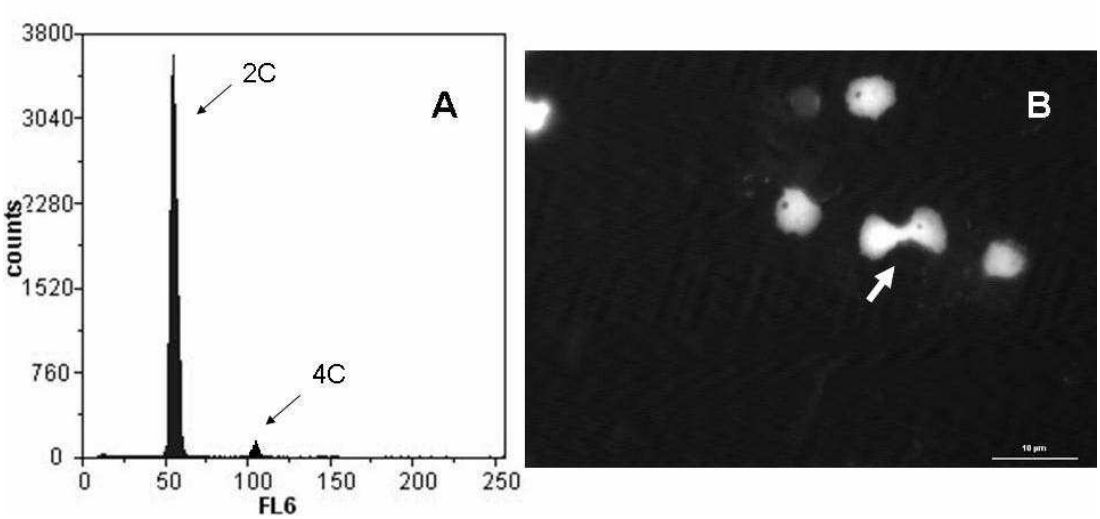
3800
3040
2280
1520
760
0
counts
2C
4C
A
0
50
100
150
200
250
FL6
B

Figure 4.

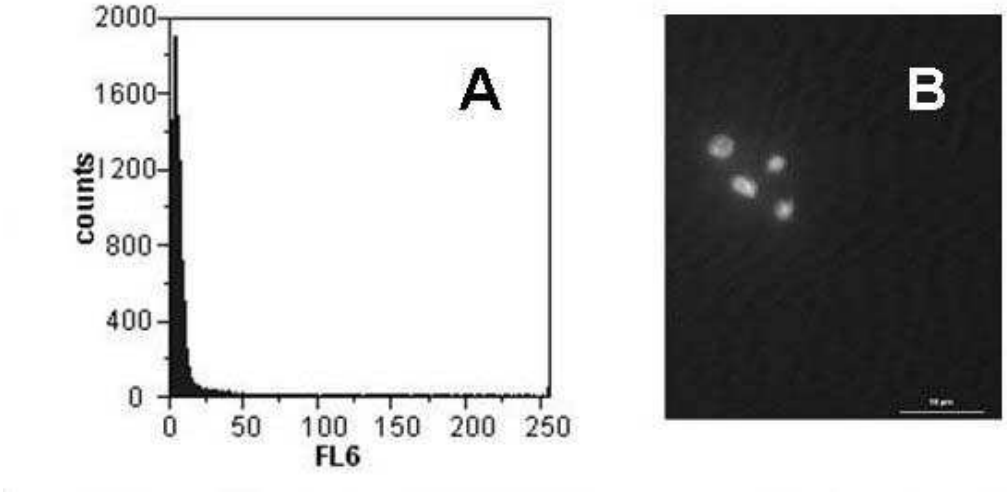

Figure 5.

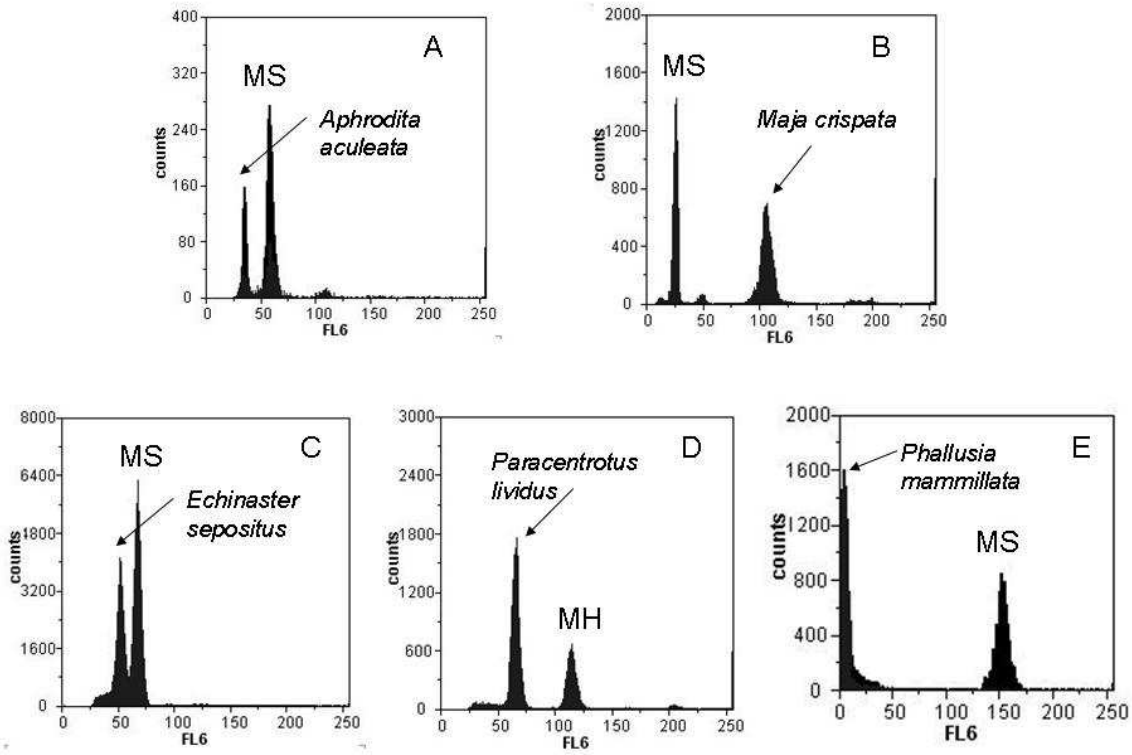
A
MS
Aphrodita aculeata
counts
FL6
B
MS
Maja crispata
C
MS
Echinaster sepositus
D
Paracentrotus lividus
MH
E
Phallusia mammillata
MS

Figure 6.